32nd Annual International Conference of the IEEE EMBS
Buenos Aires, Argentina, August 31 - September 4, 2010

Automatic Colon Polyp Flagging via Geometric and Texture Features

Marcelo Fiori,[1] Pablo Musé,[1] Sergio Aguirre,[2] and Guillermo Sapiro[3]
1. Universidad de la República-Uruguay, 2. Echopixel, 3. University of Minnesota

***Abstract*— Computer Tomographic Colonography, combined with computer-aided detection (CAD), is a promising emerging technique for colonic polyp analysis. We present a CAD scheme for polyp flagging based on new texture and geometric features that consider both the information in the candidate polyp location and its immediate surrounding area, testing multiple sizes. The proposed algorithm is tested with ground truth data, including flat and small polyps, with very promising results.**

***Index Terms*— Virtual Colonoscopy, CT Colonography, computer-aided detection, colonic polyp detection.**

I. Introduction

Colorectal cancer is the second leading cause of cancer-related deaths in the United States (only surpassed by lung cancer), and the third cause worldwide. The early detection of polyps is fundamental, allowing to reduce mortality rates up to 90%. Nowadays, optic colonoscopy (OC) is the most used detection method because of its relative high performance. However, this technique is invasive, very expensive, and still prone to miss polyps, making it hard to use in large screening campaigns.

The Computer Tomographic Colonography (CTC), or Virtual Colonoscopy, is a promising alternative technique that emerged in the 90's. It uses volumetric Computed Tomographic data of the cleansed and air-distended colon. It is less invasive and less expensive than optical colonoscopy, and as a consequence, much more suitable for screening campaigns. It also has the potential to outperform OC, in particular for small or flat polyps, or those in certain regions of the colon where OC has been shown to perform poorly.

Nevertheless, it takes more than 15 minutes for a trained radiologist to complete a CTC study, and the performance of the overall optical colonoscopy is still better. In this regard, Computer-Aided Detection (CAD) algorithms can play a key role, assisting the expert to both reduce the procedure time and improve its accuracy.

Colon lesions can be classified according to their size, measured in diameter; and according to their morphology, into pedunculated, sessile, or flat. Flat lesions are of special interest because these are an important source of false negatives in CTC, and they are around 10 times more likely to contain high-grade epithelial dysplasia [1], [2], [3].

The goal of the work presented in this paper is to flag colon regions with high probability of being polyps. Toward this aim, we introduce geometrical and textural features that take into account not only the candidate polyp region, but the surrounding area as well. For each region, several sizes are explored. This way, our proposed CAD algorithm is able to precisely detect candidate polyps by measuring local variations of these features.

The rest of the paper is organized as follows. In Section II we briefly review prior work. In Section III we introduce our proposed CAD method. In Section IV we describe the evaluation method and results. We conclude in Section V.

II. CAD Virtual Colonoscopy today

Automatic polyp detection is a very difficult problem, not only because the polyps can have different shapes and sizes, but also because they can be located in very different surroundings. Most of the previous work on CAD of colonic polyps is based on geometric features, some of them use additional CT image density information, but none of them takes into account the (geometric and texture) information of the tissues around the polyp. This is a crucial issue since it is well known that the tissue properties of the colon vary with location. This is part of the contribution of this work.

Early work on CAD methods by Vining *et al.*, [4] is based on the detection of abnormal wall thickness. Summers *et al.*, [5], detect polyps greater than $10mm$ by computing mean curvatures and sphericity ratio, and present results over a large screening patient population. Yoshida *et al.*, [6], use the Shape Index and Curvedness as geometric features, applying fuzzy clustering and then using directional gradient concentration to reduce false positives. Paik *et al.*, [7], also use geometrical features, but computing the Surface Normal Overlap (SNO) instead of calculating curvatures. Wang *et al.*, [8], compute a global curvature, extract an ellipsoid, and analyze morphological and texture features on this ellipsoid. They reach a 100% sensitivity with a relative low FP rate, using heuristic thresholds and improvable texture features. Hong *et al.*, [9], map the 3D surface to a rectangle, use 2D clustering, and reduce false positives with shape and texture features. Sundaram *et al.*, [10], compute curvatures via the Smoothed Shape Operators method, and use principal curvatures and Gaussian curvatures to detect polyps. Götkürk *et al.*, [11], propose a technique to reduce the false positives based on features calculated from three random orthogonal sections, and then classifying with SVM. Proprietary algorithms, [12], [13], have been reported as well, but with no better results than the methods listed above. However, the comparison is delicate since different databases were used.

The main goal we are addressing in this paper is to highlight/flag all the candidate polyps, so the radiologist can quickly check them. It is crucial to minimize the false negatives, keeping a reasonable false positives number. We achieve this by a two-step process: in the first one we perform a multiscale search of candidates in order to capture the appropriate polyp size, and in the second one we use

the proposed differential geometry and textural features to eliminate false positives.

III. Feature Extraction

For each case study, we consider as input both the CT images and the segmentation of the colon volume (i.e., a 3D image whose values are 1 inside the colon and zero outside). We smooth this image with a Gaussian filter and then extract the surface of the colon, using the marching cubes algorithm [14]. The result is a triangulated surface $\mathcal{S}$.

The first stage of the CAD algorithm consists in detecting surface patches that are candidates of being polyps. The complete set of connected points that constitutes the candidate patch is found growing the patch and keeping the one that maximizes the geometric dissimilarity with the surrounding area, in the sense of the features presented below (the starting point for this growth is also detailed below).

It is important to analyze the context in which the candidate patch is located, not only because different sections of the colon present different characteristics, but also because polyps can be situated over different structures such as folds or plain colonic wall. In this regard, most of the features described below take into account the local information of the area around the candidate patch. Polyps are then characterized not only by their intrinsic geometry and structure, but also by their relationship with the surrounding area.

A. Geometrical features

A good measure of the local shape of a surface is the so-called *Shape Index* [15]

$$S := -\frac{2}{\pi}\arctan\left(\frac{\kappa_{max}+\kappa_{min}}{\kappa_{max}-\kappa_{min}}\right),$$

where κ_{max} and κ_{min} are the principal curvatures computed from $\mathcal{S}$. A complementary measure called *curvedness* C, is defined as

$$R := \sqrt{\frac{\kappa_{max}^2+\kappa_{min}^2}{2}} \quad , \quad C := \frac{2}{\pi}\ln R$$

Under this coordinate transformation, the $(\kappa_{max}, \kappa_{min})$ plane is transformed into the (S, C) plane. While the value of S is scale-invariant and measures the local shape of the surface, the value of C indicates how pronounced it is. Figure 1 shows different shapes and their corresponding Shape Index. Due to the chosen orientation, Shape Index values close to -1 are of special interest for polyp detection.

Considering the Shape Index as a function $S : \mathcal{S} \to \mathbb{R}$, for each local minimum x_0 of S, the level sets around x_0 are tested as candidate patches, and the level set that maximizes the distances between the histograms described below, is the final considered patch.

Given a candidate patch $\mathcal{P}$, a ring $\mathcal{R}$ around $\mathcal{P}$ is calculated, in order to consider geometrical measurements with respect to the area surrounding the patch. The ring is calculated by dilating the patch $\mathcal{P}$ a certain geodesic distance. The geodesic distance computation is made using the algorithm in [16]. Figure 2 shows a candidate patch (actually a true polyp), and its corresponding ring. Histograms of the Shape Index values are then computed for the patch $\mathcal{P}$ and the ring $\mathcal{R}$, and two different distances between them are computed: the L_1 distance and the symmetric Kullback-Leibler divergence. These two features measure the geometric local variation of the candidate patch $\mathcal{P}$. We assume that there are no other polyps in R or that they do not significantly affect the statistics on the ring.

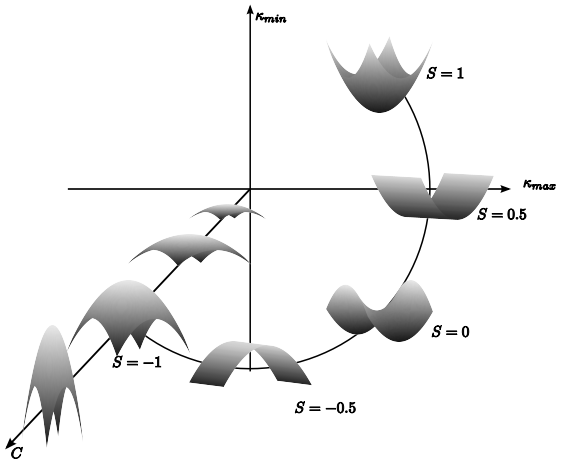

Fig. 1. Some shapes and their corresponding *Shape Index* values.

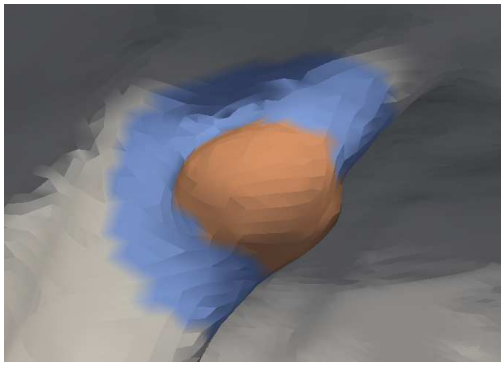

Fig. 2. Ring (in blue) surrounding a candidate polyp (in orange).

Additionally, three different variance values for the smoothing Gaussian filter are used[1], in order to obtain three different surfaces when applying the marching cubes algorithm to each one of the filtering results. The original patch is projected to these surfaces, and the mean values of the respective Shape Index computation are three additional multiscale geometric features.

Finally, the Shape Factor of the patch is also considered, defined as $SF := \frac{4\pi \cdot Area}{Perimeter^2}$. This feature allows to favor circle-like patches (like the polyp patch in Figure 2), avoiding elongated patches (like the false positives in folds).

We then end-up with a total of 6 geometric features for detecting candidate polyps, namely: L_1 and Kullback-Leibler distance between Shape Index histograms of patches and corresponding rings, the three mean values of Shape Index computed with different Gaussian filters, and the Shape Factor.

[1]the original one, $(0.75, 0.75, 0.75)$, and two more, $(0.25, 0.25, 0.25)$ and $(1.25, 1.25, 1.75)$.

B. Texture features

Due to the differences in biological activity of polyp cells, the gray-level of the CT image and its texture can be very helpful for detecting polyps. Some work has been done on the inclusion of texture features (inside the candidate polyps only), in order to reduce false positives [8]. According to the results reported there, there is a lot of room for improvement in texture features. We propose both the use of new texture features and the inclusion of the information on the candidate's surrounding area.

First, for each polyp candidate $\mathcal{P} \subset \mathcal{S}$, a volume V_1 is calculated, containing the patch $\mathcal{P}$ and a portion of the inner tissue next to the patch. A second volume V_2, surrounding V_1 is calculated, containing normal tissue, in order to compare it with the polyp candidate tissue.

The features chosen are a subset of the classical Haralick texture features [17], namely, entropy, energy, contrast sumMean, and homogeneity. Seven co-occurrence matrices (considering seven directions in $\mathbb{R}^3$, $(1,0,0), (0,1,0), (0,0,1), (1,0,1), (1,1,0), (0,1,1)$ and $(1,1,1)$) are calculated with the voxels of V_1, and all the five features are averaged over the seven directions. The analogous computation is made for V_2, and the differences between the two volumes, for each texture feature, is considered. Additionally, the mean gray levels of the voxels in both volumes is computed, and their difference is considered as a feature. In this way, six texture features are considered. This approach for computing the texture features, measuring differences with the surrounding area, leads to better discrimination than the features computed just for V_1, as demonstrated next.

IV. Experimental Results

Ten cases of the WRAMC database were used to test the proposed CAD algorithm,[2] with 19 polyps detected by optical colonoscopy, including two flat polyps. Among these 19 polyps, just one is $13mm$ in size, and the other 18 are between $4mm$ and $10mm$ in size.

At the first stage, around 1300 candidates patches were extracted (including the 19 polyps). For the purpose of classifying them with classical machine learning techniques, while dealing with the class imbalance problem, two approaches were considered: the synthetic over-sampling technique (SMOTE [18]) and Cost-Sensitive learning [19].

Although SMOTE is widely used, even in medical applications [20], we have observed that it artificially increases the performance of the classifier. For example, generating five features with random values ($\mathcal{N}(0,1)$ for both classes), and classifying with Naive Bayes, values of Area Under the ROC Curve of almost 0.8 were reached (when 0.5 was expected, as the features were independent and identically distributed).

In order to get more realistic results, we chose Cost-Sensitive learning for training and evaluating the classifier. The relative cost of false positives with respect to false negatives is chosen as the minimum value that ensures 100% sensitivity. The numerical results listed below were obtained by classifying with SVM, after normalizing the data; Naive Bayes performed similarly.

Using the leave-one-out strategy (i.e., testing with one case and training with the rest) all the 19 polyps were detected with an average of 6.6 FP per patient case. Considering that the false positives caused by segmentation errors are not direct "responsibility" of the CAD algorithm, the number of FP reduces to 3.2. In this evaluation scenario, the average number of FP per polyp was 3.5 (1.7 FP per polyp, without considering those due to segmentation errors). These values are comparable with the state-of-the-art results (same order). A more precise comparison of results is pointless, since in general each work considers its own database.

	Texture features	
	Absolute	Differential
Sensitivity	95%	100%
FP per case (all)	7.5	6.6
FP per case (excluding seg. errors)	4.1	3.2

TABLE I
COMPARISON OF ABSOLUTE AND DIFFERENTIAL TEXTURE FEATURES.

Table I shows the comparison between absolute and differential texture features. The classification was performed using all the geometric features and either the absolute texture features (computed just for V_1), or the differential texture features, using the leave-one-out strategy. The results show that, when combined with the differential geometric features, differential texture features are significantly more discriminative than the absolute ones.

A. Geometric and texture importance

Although the geometrical features are the most discriminative ones, the texture still plays a fundamental role in the classification. Indeed, adding the texture features to the geometric ones, the sensitivity reaches 100%, and at the same time the false positives rate decreases 35%.

Figure 3 shows a detected polyp, where the geometry is crucial, because the gray-level does not present considerable local variations. This is specially true in polyps located over tagged material. On the other hand, in the flat polyp of Figure 4, the geometry is weakly discriminating (although the measure considering the ring enhances the detectability), and the texture features lead to a correct classification.

Texture information is very important also because it is more robust to segmentation errors, as the texture features are computed integrating from the volumetric data itself (once the local volumes have been considered). Moreover, the differential texture features (the differences between V_1 and V_2), outperform the absolute texture features (just computed in V_1), as shown in Table I.

B. Qualitative analysis of False Positives

In addition to the number of false positives, it is very important to study how these FP patches look, since some of them can be quickly ruled out by the expert and some can

[2]Data provided courtesy of Dr. Richard Choi, Virtual Colonoscopy Center, Walter Reed Army Medical Center.

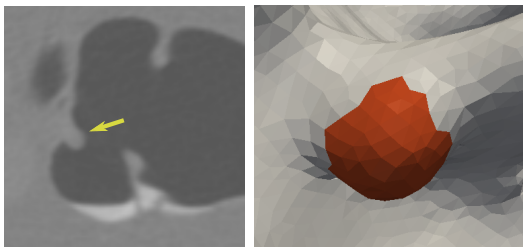

Fig. 3. Polyp with no texture information.

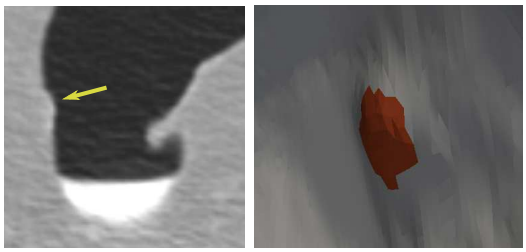

Fig. 4. Polyp with texture information, but weak geometric information.

be avoided by improving the segmentation step. About half of the false positives were caused by segmentation errors, like the ones in Figure 5. About a 10% were in fold sections of the wall, Figure 6, and another 10% were parts of the insufflation tube. The rest of the false positives are quite reasonable, in the sense that they are sections of the colon that are polyp-like shaped, Figure 6.

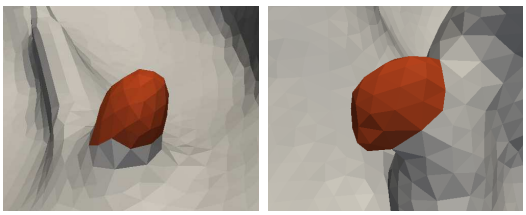

Fig. 5. False positives due to clear segmentation errors.

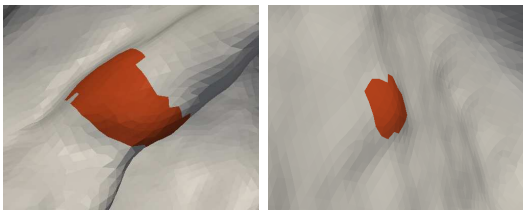

Fig. 6. False positives: fold and patch similar to flat lesion.

V. Conclusions

We introduced a CAD algorithm for candidate polyp flagging based on new geometric and texture features. In addition to the incorporation of the Haralick texture features, the main novelties of this work are in the consideration of the surrounding area for each candidate polyp (we compute differential features instead of absolute ones), and the strategy of testing regions of multiple sizes. Differential features are significantly more discriminative than the absolute features, as they emphasize local deviations of the geometry and texture over the colon. Testing regions of different sizes allows to precisely delimitate polyps. The obtained quantitative results are very promising, detecting 100% of the true-polyps, including flat and small ones. Improvement of the segmentation and, in collaborations with radiologists, finding features that are tailored to polyp-like geometries, can further improve these results.

References

[1] J. L. Fidler, C. D. Johnson, R. L. MacCarty, T. J. Welch, A. K. Hara, and W. S. Harmsen, "Detection of flat lesions in the colon with CT colonography," *Abdom Imaging*, vol. 27, no. 3, pp. 292–300, 2002.

[2] J. Fidler and C. Johnson, "Flat polyps of the colon: accuracy of detection by CT colonography and histologic significance," *Abdom Imaging*, vol. 34, no. 2, pp. 157–71, 2009.

[3] R. A. Wolber and D. A. Owen, "Flat adenomas of the colon," *Hum Pathol*, vol. 22, no. 1, pp. 70–4, 1991.

[4] D. Vining, Y. Ge, D. Ahn, and D. Stelts, "Virtual colonoscopy with computer-assisted polyps detection," *Computer-Aided Diagnosis in Medical Imaging Elsevier Science B. V.*, pp. 445–452, 1999.

[5] R. M. Summers, J. Yao, P. J. Pickhardt, M. Franaszek, I. Bitter, D. Brickman, V. Krishna, and J. R. Choi, "Computed tomographic virtual colonoscopy computer-aided polyp detection in a screening population," *Gastroenterology*, vol. 129, no. 6, pp. 1832–44, 2005.

[6] H. Yoshida and J. Näppi, "Three-dimensional computer-aided diagnosis scheme for detection of colonic polyps," *IEEE Trans Med Imaging*, vol. 20, no. 12, pp. 1261–74, 2001.

[7] D. S. Paik, C. F. Beaulieu, G. D. Rubin, B. Acar, R. B. Jeffrey, J. Yee, J. Dey, and S. Napel, "Surface normal overlap: a computer-aided detection algorithm with application to colonic polyps and lung nodules in helical CT," *IEEE Trans Med Imaging*, vol. 23, no. 6, pp. 661–75, 2004.

[8] Z. Wang, Z. Liang, L. Li, X. Li, B. Li, J. Anderson, and D. Harrington, "Reduction of false positives by internal features for polyp detection in CT-based virtual colonoscopy," *Med Phys*, vol. 32, no. 12, pp. 3602–16, 2005.

[9] W. Hong, F. Qiu, and A. Kaufman, "A pipeline for Computer Aided Polyp Detection," *IEEE Transactions on Visualization and Computer Graphics*, vol. 12, no. 5, pp. 861–868, 2006.

[10] P. Sundaram, A. Zomorodian, C. Beaulieu, and S. Napel, "Colon polyp detection using smoothed shape operators: preliminary results," *Med Image Anal*, vol. 12, no. 2, pp. 99–119, 2008.

[11] S. B. Götkürk, C. Tomasi, B. Acar, C. F. Beaulieu, D. S. Paik, R. B. Jeffrey, J. Yee, and S. Napel, "A statistical 3-D pattern processing method for computer-aided detection of polyps in CT colonography," *IEEE Trans Med Imaging*, vol. 20, no. 12, pp. 1251–60, 2001.

[12] L. Bogoni, P. Cathier, M. Dundar, A. Jerebko, S. Lakare, J. Liang, S. Periaswamy, M. E. Baker, and M. Macari, "Computer-aided detection (CAD) for CT colonography: a tool to address a growing need," *Br J Radiol*, vol. 78, no. suppl_1, pp. S57–62, 2005.

[13] S. A. Taylor, S. Halligan, D. Burling, M. E. Roddie, L. Honeyfield, J. McQuillan, H. Amin, and J. Dehmeshki, "Computer-assisted reader software versus expert reviewers for Polyp Detection on CT Colonography," *Am. J. Roentgenol.*, vol. 186, no. 3, pp. 696–702, 2006.

[14] W. E. Lorensen and H. E. Cline, "Marching cubes: A high resolution 3D surface construction algorithm," in *SIGGRAPH '87: Proceedings of the 14th annual conference on Computer graphics and interactive techniques*, (New York, NY, USA), pp. 163–169, ACM, 1987.

[15] J. J. Koenderink, *Solid shape*. Cambridge, USA: MIT Press, 1990.

[16] R. Kimmel and J. A. Sethian, "Computing geodesic paths on manifolds," in *Proc. Natl. Acad. Sci. USA*, pp. 8431–8435, 1998.

[17] R. M. Haralick, K. Shanmugam, and I. Dinstein, "Textural features for image classification," *Systems, Man and Cybernetics, IEEE Transactions on*, vol. 3, no. 6, pp. 610–621, 1973.

[18] N. Chawla, K. Bowyer, L. Hall, and W. Kegelmeyer, "Smote: Synthetic minority over-sampling technique," *Journal of Artificial Intelligence Research*, vol. 16, pp. 321–357, 2002.

[19] C. Elkan, "The foundations of cost-sensitive learning," in *In Proceedings of the Seventeenth International Joint Conference on Artificial Intelligence*, pp. 973–978, 2001.

[20] M. E. Celebi, H. A. Kingravi, B. Uddin, H. Iyatomi, Y. A. Aslandogan, W. V. Stoecker, and R. H. Moss, "A methodological approach to the classification of dermoscopy images," *Comput Med Imaging Graph*, vol. 31, no. 6, pp. 362–73, 2007.